Dynamics of Specific Vesicle-Substrate Adhesion: From Local Events to Global Dynamics

Ellen Reister-Gottfried,[1] Kheya Sengupta,[2] Barbara Lorz,[3] Erich Sackmann,[3] Udo Seifert,[1] and Ana-Sunčana Smith[1,*]

[1]*II. Institut für Theoretische Physik, Universität Stuttgart, D-70550 Stuttgart, Germany*

[2]*Centre Interdisciplinaire de Nanosciences de Marseille (CINaM/CNRS-UPR3118), Marseille Cedex 9, France*

[3]*E22 Institut für Biophysik, Technische Universität München, D-85748 Garching, Germany*

(Received 30 April 2008; published 13 November 2008)

We present a synergistic combination of simulations and experimental data on the dynamics of membrane adhesion. We show that a change in either the density or the strength of the bonds results in very different dynamics. Such behavior is explained by introducing an effective binding affinity that emerges as a result of the competition between the strength of the chemical bonds and the environment defined by the fluctuating membrane.

DOI: 10.1103/PhysRevLett.101.208103 PACS numbers: 87.16.D−, 87.15.kp, 87.16.A−

Adhesion of living cells is an immensely complex process, mediated by a bewildering variety of specific adhesion proteins (ligand-receptor pairs) [1]. It is controlled tightly by active intracellular signaling pathways that are still being elucidated [2], mostly by probing cell spreading on functionalized surfaces. Here cells first flatten locally [3,4] and establish initial contacts that are often intermittent [3] due to membrane fluctuations [5]. Cells then undergo global shape deformation concomitant with a nearly monotonous increase in the contact area [4,6–11]. Ultimately, through an actively controlled process, fully mature focal adhesions are established [2].

Unlike for mature adhesion, experimental data for the first stages of spreading are scarce but indicate that (i) spreading sometimes proceeds by expansion-retraction cycles [7], and (ii) growth until saturation of the contact area is typified by one [8,10,11], or more [4,6] power-law regimes. It is suggested that this seemingly universal behavior relies on the competition between bond formation and cell-body deformation [9–11]. However, a credible consensus based on physical principles has yet to emerge.

Elements of this physical framework were identified [12] and vindicated both in the context of cells [1] and of cell-mimetic giant vesicles ([13] and references therein). The latter are ideal for a proof-of-principle approach as vesicles spreading on substrates are simpler, yet capture many aspects of cell adhesion. Most striking is the cooperative nature of bond formation, which leads to the spontaneous formation of adhesion domains. At a low concentration of ligands in the vesicle (diffusion-limited adhesion), the area of domains was found to grow linearly in time [14–17]. In the reaction-limited adhesion (large ligand concentrations) a variety of scaling modes were suggested [14–16,18], exposing the lack of a common stance, already on the level of a passive vesicle process.

Importantly, adhesion domains are always found to grow radially, with small perturbations of radii larger than the nucleation size [17]. As will be shown herein, this result is a consequence of the exclusive use of *intrinsically strong* ligand-receptor pairs typifying all dynamical studies with vesicles and cells conducted so far. Here we focus on the reaction-limited adhesion of vesicles [19–21], which contain an abundance of sialyl-LewisX (sLex) ligands. The latter have an *intrinsically low affinity* [22] to E-selectin receptors (Esel) immobilized on a substrate (~3200, 1600 or 800 molecules/μm^2).

Changing the density of Esel induces both drastic variations in the adhesion dynamics and strong deviations from radial growth. We introduce an effective binding affinity that consists of the intrinsic chemical bond-strength v_0 and a competing term dependent on the environment. By this, we show that a decrease of the Esel density effectively decreases the affinity for sLex-Esel binding, strongly impacting the adhesion process.

We complement our experiments with simulations of reaction-limited adhesion dynamics of fluctuating membrane segments (Fig. 1). These segments contain 64 binders placed on a 640 × 640 nm square lattice [21,23]. Each ligand-receptor bond is assigned binding and unbinding rates that explicitly depend on v_0, time and the membrane-substrate distance [24]. We show that decreasing the intrinsic strength ($v_0 = 1$–$10 k_B T$), while keeping the bond environment constant (membrane properties, temperature and density of bonds), results in a similar decrease in the effective affinity as does changing the bond environment while keeping v_0 constant in the experiments. Consequently, the variations in the growth dynamics are reproduced, confirming the competitive nature of the two parts comprising the effective affinity.

The effective binding affinity.—Most generally, the binding affinity E_a is defined as the change in free energy

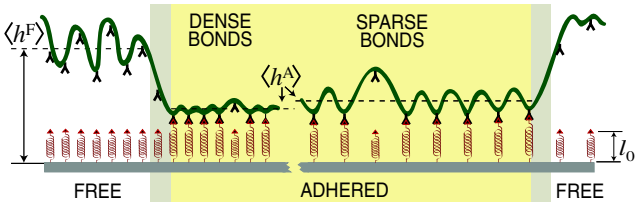

FIG. 1 (color online). An adhering membrane.

due to the formation of a bond. Equivalently, $E_a = k_B T \ln(k_{on}/k_{off})$. Here k_{on} and k_{off} are Kramers' binding and unbinding rates representing the probability that the bond is or is not formed, respectively. If one or both of the binding partners are in solution, E_a is given by the depth υ_0 of the free energy well plotted along the reaction coordinate [24]. Confining the binding partners to two opposing surfaces decreases the binding and increases the unbinding probability when the surfaces are set to larger h separations [24]. Consequently, E_a becomes distance dependent.

In the case of a flat substrate interacting with a vesicle membrane, the separation $h(r, t)$ varies in time t and space r, due to membrane fluctuations and local forces exerted on the membrane (Fig. 1). Therefore, k_{on} and k_{off}, as well as E_a, are also local, time-dependent properties that should be defined on the level of a bond. By assuming that a bond at the position r_i, is a harmonic spring with a constant k, which can be stretched from its rest length l_0, and under conditions of detailed balance, the effective binding affinity of a bond is $E_a^{\text{bond}}(r_i, t) = \upsilon_0 - k[h(r_i, t) - l_0]^2/2$. Here the first term is the intrinsic binding affinity, whereas the second, harmonic term depends on the local position of the membrane, and thus accounts for the elastic properties of the membrane and its fluctuations indirectly (Fig. 1). In our simulations this definition is exact, whereas in experiments, the harmonic term is the first order correction.

One can average over all positions within a region to obtain the binding affinity of that region $E_a^{\text{state}} = \upsilon_0 - k\langle[h(r_i) - l_0]^2\rangle/2$. If, at a given instance of time, the height of a membrane is almost uniform within such region, averaging over all positions can be approximated by averaging over the membrane conformation: $E_a^{\text{state}} \simeq \upsilon_0 - k(\langle h^{\text{state}}\rangle - l_0)^2/2$. In adhering vesicles, such regions are the interior of the adhesion domains (state $= A$) and the freely fluctuating membrane in the remainder of the contact zone (state $= F$), where furthermore, the mean heights are found to be time independent. Because of $\langle h^F\rangle > \langle h^A\rangle$, one gets $\langle k_{off}^F\rangle \gg \langle k_{off}^A\rangle$ and $\langle k_{on}^F\rangle < \langle k_{on}^A\rangle$. As a result, $E_a^F \ll E_a^A$.

The adhered and the free states comprise the majority of the binders. The two states are separated by a rim (Fig. 1) where the membrane, controlled by its elasticity and fluctuations, gradually changes height from the domain edge at $\langle h^A\rangle$ to $\langle h^F\rangle$. The height of a membrane profile at which υ_0 equals the spring contribution, defines a critical distance from the domain edge. This distance characterizes the lateral width of the moving front where the events that govern the domain growth take place.

Nucleation.—Initially, the vesicle sediments down to the minimum of a weak membrane-substrate potential, about 100 nm above the substrate, where a strongly fluctuating contact zone is created (the free state). Although the incorporation of binders allows for specific adhesion, the affinity E_a^F at this height is such that the formation of bonds is rendered almost impossible. It is the fluctuation-induced approach of the membrane to the substrate occurring simultaneously with ligand-receptor interaction (promoted by υ_0) that is entirely responsible for the formation of the first bond(s). The first bond(s) deforms the membrane and keeps it close to the substrate, locally elevating the effective affinity. This allows the establishment of further bonds with a strong preference for the vicinity of the first bond (s)—we term this the ''neighbor effect.'' An increase in receptor density leads to denser packing of bonds and a mean profile of the membrane that is, on average, closer to the substrate than when the bonds are sparse (Fig. 1). Furthermore, the fluctuations, which pull and unbind formed bonds, are more efficiently suppressed. Hence, stronger neighboring effects (larger E_a^A,) occur with greater density of binders and the nucleation is thus faster. Nucleation of a domain marks the onset of the adhered state, seen in RIC-micrographs as a dark, nonfluctuating patch. The development of domains that follow nucleation is mediated by the formation of membrane patches (500 nm in size), henceforth called speckles. In all investigated systems, speckles adhere or de-adhere with their entire area at once, but independently of each other.

The above reasoning is fully supported by our simulations that model the adhesion process of a single speckle. There, no stable adhesion is achieved if fluctuations in the free state ($h = 120$ nm) are suppressed, or the membrane is not allowed to deform. Indeed, the formation of the first bond is facilitated by membrane deformability and fluctuations as well as by stronger υ_0. Moreover, larger υ_0 is associated with the stronger neighbor effect, simply because the bonds have longer lifetimes and pull more strongly on the membrane.

Local events.—The effective binding affinity concept can be applied to all experiments reported so far. For example, large υ_0 such as in biotin-avidin bonds ($\upsilon_0 = 35k_BT$), completely dominates the harmonic term in E_a^A. This leads to a prompt nucleation after which the strong neighbor effect drives the fast, radial movement of the narrow domain front [15]. The high velocity of the front ensures that the adhesion is complete before a competing nucleation patch is formed. When a weaker integrin-RGD pair ($\upsilon_0 = 10k_BT$) is used, the intrinsic term in E_a^A still dominates, but the spring term starts to play a role. Consequently, the adhesion process is slower, more domains have time to form, and the perturbations of the moving front are larger [25].

In the present case of sLex-Esel binding, υ_0 is further decreased to $\sim 5k_BT$, providing true competition with the harmonic term in E_a^A. The radial growth is perturbed to length scales typical for nucleation and the moving front is decomposed into speckles. After a speckle (dis)appears, the domain-edge stands still before restarting in another direction or at a different section of the domain-edge. The time between individual movements increases notably with decreasing the Esel coverage, as the neighbor effect is suppressed. Single speckle formation occurs over a time scale of seconds and is seen in RICM as tapping of the membrane close to the substrate.

At low Esel coverage [Fig. 2(b)], speckle growth frequently induces steplike features in domain-area growth curves. Entire speckles frequently de-adhere [speckle A in Fig. 2(a)], resulting in substantial noise and occasional decline in growth curves. The adhesion process is so slow that typically 4–5 domains form and develop independently. At intermediate Esel coverage, a smaller number of domains appear, some of them merging. Speckle retractions are not so common, and the domain growth curves are less rough (data not shown). At high Esel density [Fig. 2(c)], speckle retractions are virtually nonexistent, giving rise to typically 1 or 2 domains that smoothly grow in time. Speckle formation is frequent and often several form simultaneously at various locations along the edge of a single domain. However, for small domain sizes, the data remain noisy until the domains become large and a smooth growth curve is obtained. Finally, most of the contact zone is adhered, showing that the system is near the first order "wetting" transition [14].

Since the transition from the free to the adhered state occurs locally by formation of a speckle, it can actually be simulated, which we do for various υ_0. At lower υ_0 [Fig. 3(a)] the time for the formation of first bonds is long. The unbinding of individual bonds induce large fluctuations in the total number of bonds. Occasionally, the number of bonds in the speckle drops to zero which is equivalent to a de-adhesion event. On the other hand, large υ_0 [Fig. 3(b)] leads to fast development of first stable bonds, whose number grows smoothly. Simultaneously, the average height of the membrane and its fluctuations decrease, promoting binding until the entire speckle is in the adhered state (no de-adhesion was observed). Notably, only $2k_BT$ difference in υ_0 leads to these various growth patterns, confirming the large sensitivity of the adhesion dynamics to small changes in E_a^A.

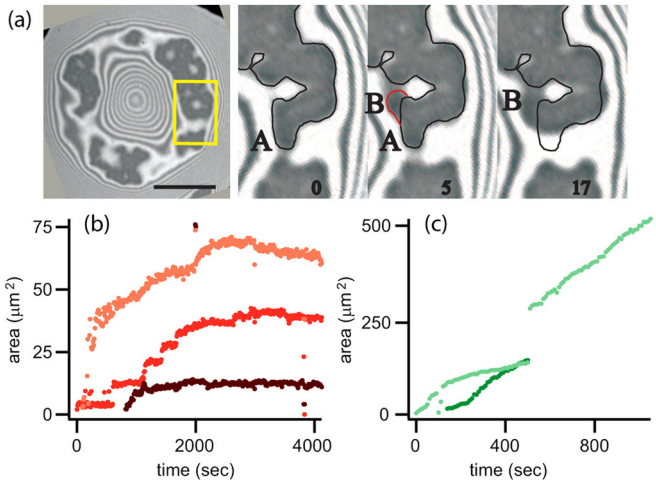

FIG. 2 (color online). (a) The contact zone with several dark adhesion domains and an inset over 3 snapshots is shown. The domain edge at $t = 0$ (thin black line) is displayed and overlayed with the insets from later times. Growth of speckle B is marked in red at $t = 5$ sec. De-adhesion of speckle A is seen at $t = 17$ sec as white area within the initial domain boundary. The scale bar shows 10 μm. (b) Growth of three domains developing on a low Esel concentration. (c) For high Esel concentration, the area of two domains merging in time.

The global dynamics emerges as a smooth process only as a result of sufficient averaging over independent local events. Experimentally, spatial averaging over speckle adhesions in the entire contact zone occurs naturally when determining the area of all domains [Fig. 4(a)]. The growth of the adhered state saturates as the equilibrium is reached (Fig. 4). The latter arises from the balance between the sLex mixing entropy and binding enthalpy within the finite vesicle geometry [13,19], and can take place before the contact zone is filled with bonds. The speckle-by-speckle domain growth is mimicked in the simulations by averaging over many (200) runs [Fig. 4(b)]. In simulations, the equilibrium is generally, but not always associated with a loss of the free state.

The affinity characterizing the ligand-receptor interaction E_a^{eq}, can be extracted from the effective binding affinity of the system in equilibrium. By definition, this is the ratio of probabilities that a bond is and is not formed: $E_a^{\mathrm{eq}} = \ln[\langle N_b\rangle/(N_{\mathrm{tot}} - \langle N_b\rangle)]$. Here $\langle N_b\rangle$ is the equilibrium number of bonds and the N_{tot} is the total number of receptors on the surface. In simulations E_a^{eq} can evidently be determined explicitly while in the experiments, equivalent reasoning provides $E_a^{\mathrm{eq}} = \ln(A^A/A^F))$, A^F and A^A being the free and adhered areas of the contact zone. For high, middle and low Esel coverage, A^A is associated with 98%, 43%, and 26% occupancy of the contact zone, which leads to an E_a^{eq} of 4.0, -0.3, and $-1.0k_BT$, respectively. The negative E_a^{eq} emerges when less than 50% of the contact zone is adhered. A similar crossover from positive to negative E_a^{eq} is obtained in simulations by decreasing υ_0. This shows that small variations in the chemical bond strength or in the environment drastically change the conditions for the specific adhesion.

We attempted to determine the time dependency of curves in Fig. 4, as was done hitherto, by fitting an exponentially saturating or a power law. At experimentally high Esel density or high υ_0 in simulations ($E_a^{\mathrm{eq}} > 0$), the linear curve is most appropriate. At medium Esel density or intermediate υ_0 ($E_a^{\mathrm{eq}} \simeq 0$), both an exponentially satu-

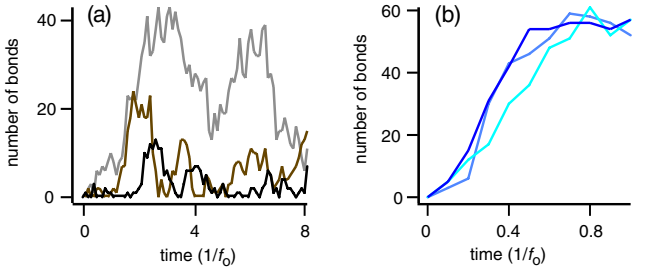

FIG. 3 (color online). Number of bonds as a function of time (set by the attempt frequency f_0 [23]). Three simulation runs are shown for (a) weak [$\exp(\upsilon_0/k_BT) = 3.0$] and (b) strong [$\exp(\upsilon_0/k_BT) = 10.0$] binding.

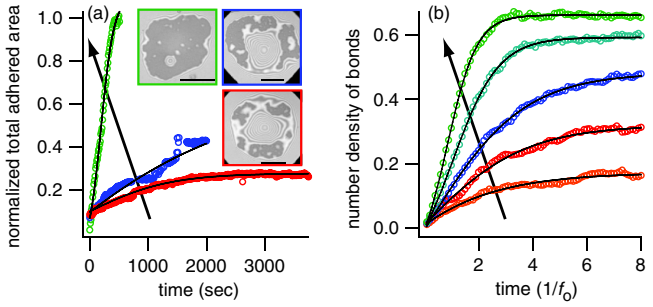

FIG. 4 (color online). (a) Adhered area (normalized by the equilibrium contact zone area) in time for vesicles on substrates with high, middle and low Esel densities. For vesicles of comparable size halving the concentration of Esel approximately doubles the equilibration time. The scale bar is 10 μm. (b) Average number of bonds in time in sets of 200 simulation runs for $\exp(v_0/k_BT) = 3.0$, 3.25, 3.5, 3.9, and 4.5. The directions of growing Esel density and v_0 are shown with arrows.

rating and a power law with an exponent <1 are good choices. At low density or low v_0 ($E_a^{\mathrm{eq}} < 0$), only the exponential provides a good fit. On the other hand, we empirically find that a hyperbolic tangent [$A(t) = C_1 \tanh(C_2 t + C_3) + C_4$] can be very well fitted to all cases (all E_a^{eq}). Here the coefficients should be nontrivial functions of the ligand and receptor densities, E_a^A, and E_a^F.

This fit allows for three phases in the adhesion dynamics: (i) the nucleation inducing a slow onset. It is dominated by the membrane free state and relies on the statistical coordination of the membrane-substrate approach and the stable bond formation; (ii) the (linear) growth which results from a fine balance between the intrinsic properties of binders and the membrane; (iii) the exponential saturation to the equilibrium driven by a single relevant time scale. The relative strength of the fitting coefficients (and the parameters that they comprise) determines how much time the system spends in one of the phases before continuously moving into the next one.

In conclusion, by revealing the statistical nature of the adhesion process, theoretically explained through the concept of the effective affinity, we have succeeded in integrating understanding of local events with the global behavior of adhering vesicles. The idea of associating local reaction rates with the adhesiveness has been successfully applied already in the context of multiple conformations of binders, where the binding rates vary due to active processes [26] rather than being environment dependent. Here, we have shown that for binders confined to surfaces and under conditions of detailed balance, the binding rates are not intrinsic properties of a binding pair, but depend sensitively on the environment. This turns out to be a very powerful tool to control adhesion. We have identified membrane fluctuations and the density of binders as one of main environmental factors that affect the nucleation and the effective binding affinity in vesicles. In the context of cells, it remains to be revealed how this affinity is used and controlled. Here too fluctuations may have an important role, as they strongly influence the early stage of the cell adhesion process [3,5].

We acknowledge DFG-SE 1119/2-1 for funding.

*Corresponding author.

[1] P. Bongrand, Rep. Prog. Phys. **62**, 921 (1999).
[2] B. Zimerman, T. Volberg, and B. Geiger, Cell Motil. Cytoskeleton **58**, 143 (2004).
[3] A. Pierres *et al.*, Biophys. J. **94**, 4114 (2008).
[4] K. Sengupta *et al.*, Biophys. J. **91**, 4638 (2006).
[5] A. Zidovska and E. Sackmann, Phys. Rev. Lett. **96**, 048103 (2006).
[6] H. Döbereiner *et al.*, Phys. Rev. Lett. **93**, 108105 (2004).
[7] B. J. Dubin-Thaler *et al.*, Biophys. J. **86**, 1794 (2004).
[8] A. Hategan *et al.*, Biophys. J. **87**, 3547 (2004).
[9] T. Frisch and O. Thoumine, J. Biomech. **35**, 1137 (2002).
[10] F. Chamaraux *et al.*, Phys. Rev. Lett. **94**, 158102 (2005).
[11] D. Cuvelier *et al.*, Curr. Biol. **17**, 694 (2007).
[12] G. I. Bell, Science **200**, 618 (1978).
[13] A.-S. Smith and U. Seifert, Soft Matter **3**, 275 (2007).
[14] A. Boulbitch, Z. Guttenberg, and E. Sackmann, Biophys. J. **81**, 2743 (2001).
[15] D. Cuvelier and P. Nassoy, Phys. Rev. Lett. **93**, 228101 (2004).
[16] F. Brochard-Wyart and P. G. de Gennes, Proc. Natl. Acad. Sci. U.S.A. **99**, 7854 (2002).
[17] V. B. Shenoy and L. B. Freund, Proc. Natl. Acad. Sci. U.S.A. **102**, 3213 (2005).
[18] P.-H. Puech *et al.*, Biophys. Rev. Lett. **1**, 85 (2006).
[19] B. G. Lorz *et al.*, Langmuir **23**, 12 293 (2007).
[20] Vesicles- DMPC: cholesterol: DMPE-PEG2000: sLex = 1:1:0.01:0.15 (lipids from AvantiPolar Lipids, USA); Substrate-extracellular part of Esel (Calbiochem, USA) is physisorbed to amino-silanized glass. Complete preparation details are given in Ref. [19].
[21] See EPAPS Document No. E-PRLTAO-101-017846 for more information on materials and methods. For more information on EPAPS, see http://www.aip.org/pubservs/epaps.html.
[22] A.-S Smith *et al.*, Biophys. J. **90**, 1064 (2006).
[23] Langevin dynamics simulations of a membrane (bending rigidity $\kappa = 10 k_B T$, $T = 300$ K) are done as in E. Reister-Gottfried, S. M. Leitenberger, and U. Seifert, Phys. Rev. E **75**, 011908 (2007), using the membrane hydrodynamic coefficient of U. Seifert, Adv. Phys. **46**, 13 (1997). Initially the membrane with no bonds is placed in a parabolic membrane-substrate potential (strength 13 J/cm^4) with a minimum at $h_0 = 120$ nm. The formation of bonds induces a movement of the membrane's center of mass as in L. C.-L. Lin and F. L. H. Brown, Biophys J. **86**, 764 (2004). The bonds are modeled as dynamic harmonic springs ($l_0 = 80$ nm, $k = 5 \times 10^{-5}$ N/m) with an attempt frequency $f_0 = 2000$/s.
[24] E. Evans and D. Calderwood, Science **316**, 1148 (2007).
[25] S. Goennenwein, M. Tanaka, and E. Sackmann, Biophys. J. **85**, 646 (2003).
[26] B. Rozycki, R. Lipowsky, and T. Weikl, Phys. Rev. Lett. **96**, 048101 (2006); B. Rozycki, T. Weikl, and R. Lipowsky, Eur. Phys. J. E **22**, 97 (2007).